University of Baghdad
College of Engineering
JOURNAL OF ENGINEERING

Journal of Engineering

journal homepage: www.jcoeng.edu.iq

Volume 30 Number 9 September 2024

Finite Element Analysis of Shear Performance for Reinforced Concrete T-Beams by Polymer Bars Strengthened with Carbon Fiber Using Embedded Through Section Technique

Hussain Hassan Alhilli *, Mahdi Hameed Al-Farttoosi

Department of Civil Engineering, College of Engineering, University of Baghdad, Baghdad, Iraq

ABSTRACT

The purpose of this research presents the research results obtained from a numerical simulation using the ABAQUS/CAE version 2019 finite element software. This study tested the shear behavior of T-beams made of reinforced concrete (RC). The structure is reinforced with a carbon fiber reinforced polymer (CFRP) bar embedded through a section (ETS). The numerical validation approach implicated using numerical analysis on the experimental data collected from twelve reinforced concrete (RC) T-beams divide into two groups each group include reference beam, the field of numerical analysis was expanded to encompass the examination of many aspects, such as the impact of the diameter of CFRP bars. The main objective of this project is to create a computational model that accurately transcribes the complex nonlinear properties inherent in beams. This work conducts a comparative investigation of computational and experimental models, with a specific focus on their load-deflection features and cracking patterns. The study found that the average ratio of ultimate load to deflections in numerical model simulations for beams was 1.011, whereas in experimental testing it was 0.928. The research findings establish a clear correlation between the diameter of CFRP bars and the stiffness of a beam, assuming a constant angle of inclination and spacing.

Keywords: T-beams; CFRP bars; Shear stresses; Embedded through section (ETS).

1. INTRODUCTION

Over of the last three and a half decades, using Carbon Fiber Reinforced Polymer (CFRP) Combined materials stiffened in reinforcing concrete parts has acquried considerable attention as an substantial method for rehabilitating infrastructure. Applications for strengthening with (CFRP) are numerous and

*Corresponding author
Peer review under the responsibility of University of Baghdad.
https://doi.org/10.31026/j.eng.2024.09.11

Article received: 16/09/2023
Article revised: 10/11/2023
Article accepted: 10/11/2023
Article published: 01/09/2024

include both creating new structures and enhancing ones that already exist. **(Mhanna et al., 2019; Naqe et al., 2020; Naqi et al., 2020; Turki and Al-Farttoosi, 2023; Abbas and Al-Zuhairi, 2023).** The general failure criteria in concrete beams, in addition to analyzing concrete beams reinforced with (CFRP), researchers have focused their efforts on studying the localized behavior that takes place at the bond interface. Considerable actions have been undertaken to establish a thorough understanding of bond behavior at the interface, which is the primary source of early failures **(Al-Farttoosi et al., 2013; Abbas et al., 2013; Izzat, 2015; Naqe and Al-Zuhair, 2020; Abdulkareem and Izzat,2022)**. A composite materials CFRP Used for improving purposes has a high degree of versatility, as it may be effectively utilized across many structural components, including beams, columns, slabs, and walls. The aims of improvement may vary according to the categorization of the person. Several aims exist to augment the load capabilities of a structure, including axial, flexural, and shear loads. Another objective is to enhance the rigidity of the structure to minimize deflections under both service and design loads. In addition, endeavors are undertaken to prolong the structural fatigue life and bolster its resilience against environmental influences **(Buyukozturk et al., 2004)**.

The shear strengthening of (RC) beams is influenced by many key elements, as identified in previous studies **(Ghadhban, 2007; Chen et al., 2019)**. These factors include (f'c), the proportion of main steel (ρ), the dimensions of the beam, the effective depth (a/d) ratio of a shear span, and the ratio of shear reinforcement (ρv). To make RC beams stronger in shear, epoxy can be used to bond FRP bars to vertical holes drilled into concrete. So far, there have not been many experiments done on how embedded through-section (ETS) FRP rods can be used to make RC beams stronger against shear. **(Chaallal et al., 2011)** showed the results of an experimental study comparing the performance of the ETS method to that of the external bond EB and near surface mounted NSM techniques. T-beams measuring 4520 mm in length undergo 12 tests in total. (1) the efficiency of the ETS technique in comparison to the EB FRP sheet and NSM rod methods; (2) the existence of the internal steel; and (3) the internal ties ratio is explored (i.e., spacing). The findings validate the viability of the ETS approach and demonstrate that the shear behavior of samples reinforced using this technique is much better than that of beams reinforced with the EB and NSM. The efficacy of the ETS approach was examined by **(Barros et al., 2013)** a detailed experimental investigation was conducted, including a total of 14 reinforced concrete (RC) beams. The results of a investigation revealed the following outcomes: (i) Inclined externally bonded textile-reinforced polymer (ETS) strengthening bars exhibited superior effectiveness compared to vertically oriented ETS bars. Furthermore, the beams' shear capacity increased as the spacing between bars decreased. (ii) The occurrence of brittle shear failure was transformed into a more desirable ductile flexural failure mode. (iii) The shear capacity of a beam displayed an increase as the spacing between bars decreased.

The suitability of the ACI 318 (2006) and Eurocode 2 (2003) requirements for shear resistance was assessed. The experimental and analytical findings exhibited a strong correspondence, indicating a high level of agreement between the two. **(Deniaud et al., 2003)** conducted a comprehensive investigation on the interplay between concrete, steel ties, and (FRP) sheets in the strengthening of RC beams under the effect of shear pressures. Eight experiments were done on four T-beams made of concrete under controlled laboratory conditions. The beams underwent a four-point loading configuration. The testing of each end

of every beam was conducted individually. The web of T-beams was externally reinforced using three kinds of (FRP): single glass fibers, single carbon fibers, and tri-axial glass fibers. However, some ends were intentionally left without FRP reinforcement. The results of experimental work where findings indicate that incorporating (FRP) reinforcement significantly enhances the maximum shear strength, ranging from 15.4% to 42.2%, compared to beams without FRP reinforcement. The shear capacity improving is contingent upon both the specific kind of fiber-reinforced polymer (FRP) material used and the quantity of internal shear reinforcement present. The triaxial glass fiber reinforced beam had a more increasing degree of ductile failure compared to the other beams reinforced with (FRP). Furthermore, this work introduces a test model grounded in a logical process with a high degree of accuracy. In experimental predicting outcomes. **(Benzeguir et al., 2019)** the demonstrated findings of an observed study accomplished on 18 (RC) T-beam specimens with different diameters.

The study is aimed to analyze the effect dimensions on the shear strength of concrete at the point of failure in (RC) beams that were strengthening in shear using (CFRP) sheets. The samples were classified into two groups, distinguished by the presence or lack of internal transverse steel (without steel stirrups). Sizes ranging from small to large were represented in the six sets of beams that were created from the three groups. Two groups of control samples were included in the series. One group of samples was reinforced in shear using a combination of EB-CFRP sheets with a single layer of fabric, and the other group of samples was reinforced in shear using a configuration of EB-CFRP sheets with multiple layers of fabric. The research shows that the width and length of concrete and CFRP sheets have a significant impact on their shear stress resistance. Reinforced samples without stirrups were more affected by size as CFRP sheet stiffness increased. The researchers mainly attributed the reduced behavioral impact in their study on reinforced beams to the correlation between the stirrups and the EB-CFRP sheets. **(Godat et al., 2013)** Two-dimensional finite element models were created to evaluate CFRP concrete and bars in an ETS test at their interface. The proposed method involves carefully positioning truss elements above or below the bar to create ties between the CFRP and the concrete layer that surrounds it. Numerical simulations using concrete-CFRP bar interface characteristics show how to calculate the ideal lengths of CFRP bars. FRP shear-strengthened beams are now part of the study. We will use the embedded through section (ETS) method and three-dimensional finite element analysis to create and test a model. Verified constitutive models replicate the nonlinear properties of CFRP bars, reinforcing steel, and concrete.

This comprehensive report covers CFRP bars' maximum load-carrying capacity, load-deflection correlations, and longitudinal stress. Compared to experimental data, numerical predictions match experimental and finite element findings. **(Qapo et al., 2016)** A three-dimensional nonlinear finite element (FE) model for reinforced concrete (RC) beams reinforced using deep embedment (DE) techniques has been developed and validated by us. We contrasted the FE and Concrete Society TR55 predictions using experimental data. The finite element (FE) study forecasts a shear strengthening improved the ratio of 1.08, together with a standard deviation of 0.249. On the other hand, the TR55 model forecasts a shear ability development ratio of 1.569, along with a standard deviation of 0.54.

A study was undertaken to investigate quantitatively using parametric methods. The study's results indicate that the expected increase in shear strength was favorably affected by the

incorporation of inclined distributed electrical fiber reinforced polymer (DE FRP) bars and the enhancement of concrete's compressive strength. Nevertheless, the level of improvement saw a decline when the ratio of shear span to depth and the ratio of the inside steel stirrup to DE FRP bar rose. The magnitude of the size effect did not significantly influence the anticipated percentage of enhancement in shear strength. **(Abbasi et al., 2022)** performed a numerical investigation to evaluate the impact of dimensions on the shear ability of (RC) beams that were reinforced in shear using externally bonded carbon fiber reinforced polymer (EB-CFRP).

Despite a limited number of experimental research, there is a shortage of finite element (FE) studies considering the size impact. Experimental testing is resource-intensive and time-consuming, rendering them incapable of comprehensively capturing the intricate and interdependent nature of the factors involved. Recently, there has been substantial advancement in creating comprehensive numerical models and fundamental principles to predict the outcomes of laboratory experiments. Recent developments have primarily concentrated on resolving concerns with the shear resistance of reinforced concrete (RC) beams. In recent times, computational simulations have made important improvements in accurately illustrating the strain profile within the fibers, the interface shear stress within the connection between them, and the established principal diagonal shear cracks.

The subject of this outlines the conclusions of a nonlinear finite element numerical analysis performed on the nine reinforced concrete (RC) beams that were reinforced in shear utilizing external bonded- carbon fiber reinforced polymer (EB-CFRP) composites. The beams were subjected to laboratory testing, with each series containing three sets of reinforced concrete beams that were geometrically equal but of varying sizes (small, medium-sized, and big). The result obtained illustrate that numerical models can correctly foresee experimental outcomes. **(Najaf et al., 2022)** analyzed and simulated the concrete beam using the finite element tool Abaqus. Some of the elements that are included in a thorough analysis are the kind, amount, and installation angle of (FRPs). In this study, twenty-five numerical models are taken into account. Glass fiber reinforced polymer (GFRP), carbon fiber reinforced polymer (CFRP), and aramid fiber reinforced polymer (AFRP) types of coverings are utilized by these models. You may get the covers in 6-sheet or 12-sheet configurations, and you can mount them at 30-, 45-, 60-, or 90-degree angles.

In order to reduce the propagation of fractures, all of the models have FRP layers at the bottom of the beam. When a constant load of 60 kN is given to all models, the stresses created in the beam and the displacement at the beam's midpoint are the primary areas of inquiry. Results show that a 45-degree installation angle for FRP sheets yields a more noticeable reduction in displacement compared to a 60-degree angle, all else being equal in terms of quantity of sheets and distance of installation. In addition, compared to a 90-degree installation, a 60-degree tilt has a far more noticeable influence. Moreover, the incorporation of plates reduces up to 12.5% in the maximum lateral strain experienced at the midpoint of the beam span. Furthermore, it can be seen that the (CFRP) material exhibited superior performance when compared to the other two fiber types. The incorporation of prestressed (FRP) sheets into the specimens results in an enhancement in their structural strength. The load increment persists until the beam reaches a critical point at which it collapses owing to the compressive concrete undergoing crushing. Introducing prestressed fiber-reinforced polymer (FRP) sheets to the specimens significantly enhances strength versus the ultimate

load, ranging from 5.4% to 26.4%. This improvement is in comparison to the beam that only relies on internal confinement provided by the internal rebars.
The research aims to determine numerically the shear behavior of RC T-beams enhanced by CFRP bars using the embedded through section (ETS) technique**.**

2. TEST SPECIMENS

The testing program from **(Alhilli and Al-Farttoosi, 2023)** tested twelve T-beams made of (RC). This included two reference beams, and ten strengthened beams not subjected to any strengthened measures. The twelve beams were categorized into two primary types: those with stirrups and those without stirrups, with just three of them including steel bars for additional support. The primary factors under investigation were CFRP bars' spacing and angle of inclination. The reinforced beams showed enhanced shear strength by inserting 12 mm CFRP bars along the central axis of the section with varying spacing and degrees of inclination. The significance of CFRP bars' spacing and inclination angle on several factors is tested, including failure load, crack distribution, load-strain connections, and load-deflection relationship. All beams within each group possess identical characteristics, namely length of 2200 mm, cross-section measurements, and reinforcement. As illustrated in **Figs. 1 and 2** every beam was subjected to a monotonic one-point load at mid-span until failure. The composition and designation of tested beams details of examined beams are given in **Table1.** The physical characteristics of concrete, such as its modulus of elasticity of 268645 MPa, compressive strength of 37.14 MPa, and tensile strength of 3.73MPa, were quantified by measurement. The average yield, ultimate strength, and elongation of steel bars were determined using standardized testing, representing CFRP by elastic, perfect plastic for stress-strain in the properties of CFRP bar. **Table 2** provides the characteristics of the adopted concrete mix and steel rebars.

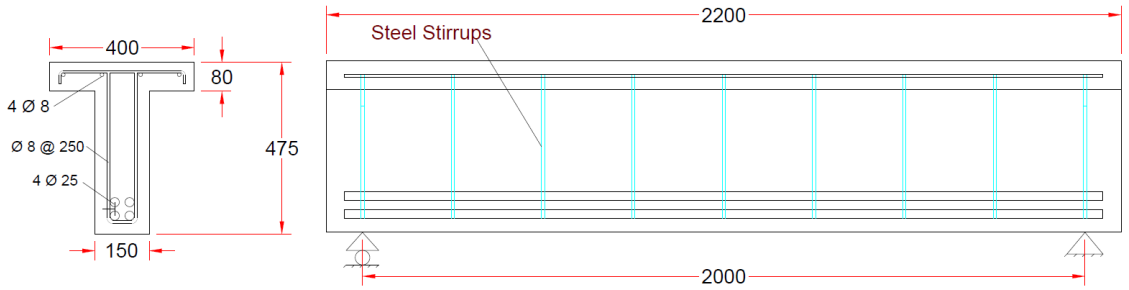

(a)

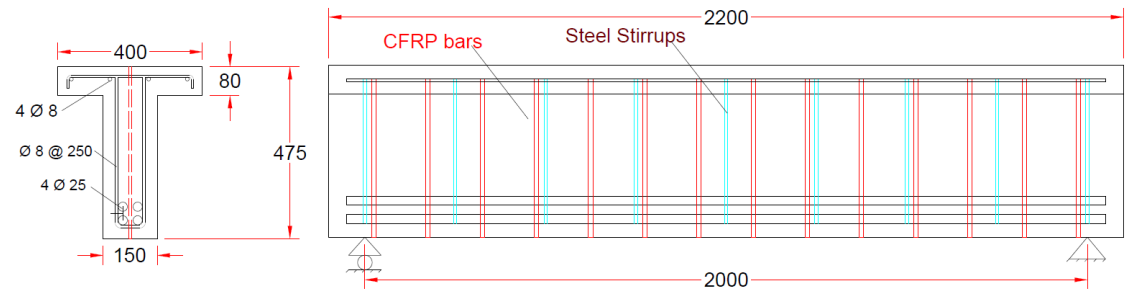

(b)

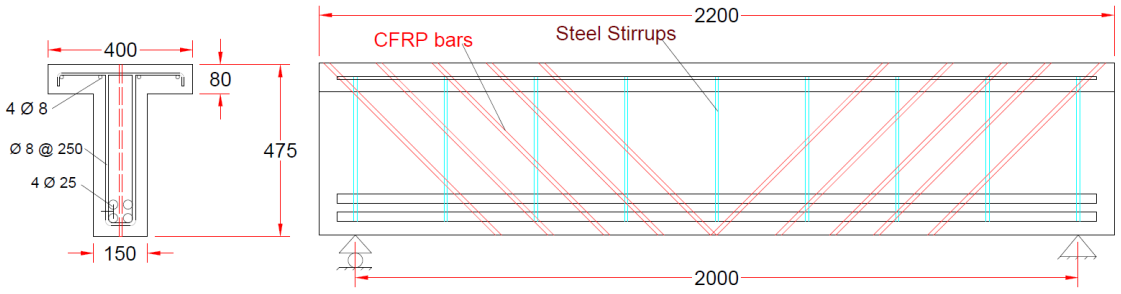

(c)

Figure 1. Details of group 1 beams with stirrups: a) Reference beam (un-strengthened), b) Strengthened beam with right angle CFRP bars, c) Strengthened beam with inclined CFRP bars.

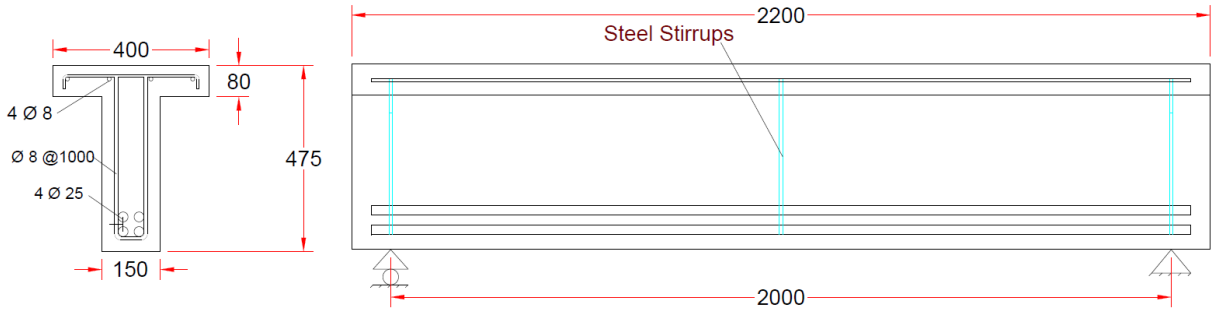

(a)

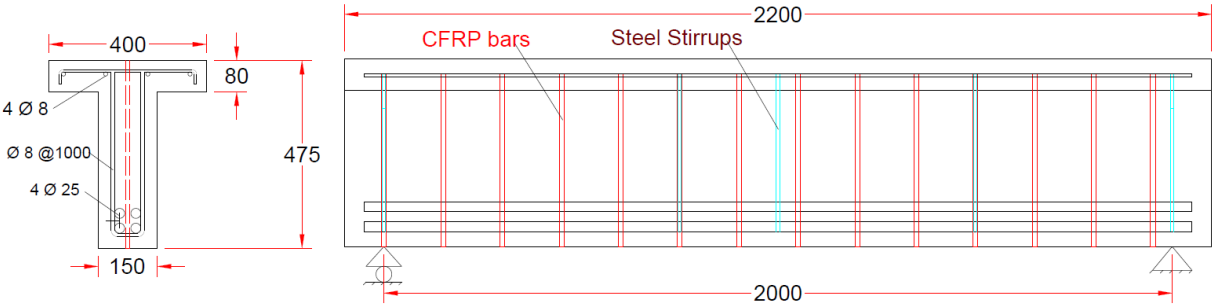

(b)

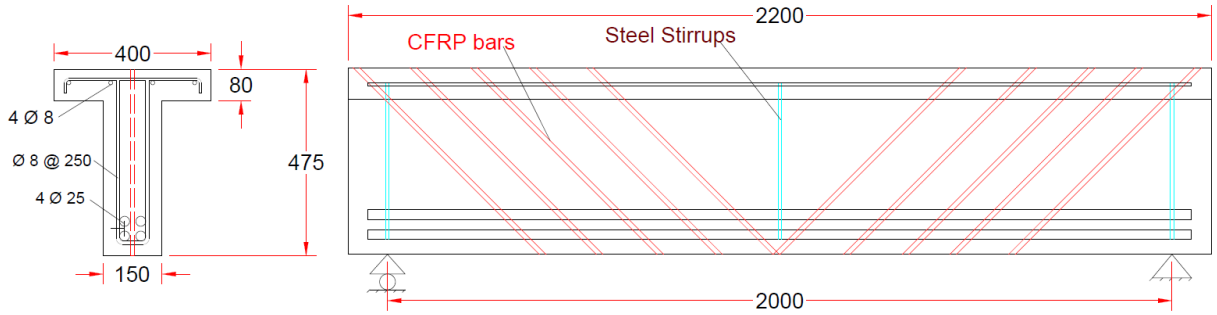

(c)

Figure 2. Details of beams for group 2 without stirrups: a) Reference beam (un-strengthened), b) Strengthened beam with right angle CFRP bars, c) Strengthened beam with inclined CFRP bars.

3. MODELING AND ANALYSIS OF TESTED BEAMS IN ABAQUS

The present research uses the Finite Element Method to analyze T-beams via implementing the ABAQUS 2019 computer program, specifically applying the Standard/Explicit Model with a mesh size of 25mm. The structural study of all beams used a single-step approach, specifically static analysis. The T-beams were simulated using the isoperimetric eight-node

Table 1. The configuration and designation of tested beams details of examined beams.

Group	Beam-ID	the angle of inclination of CFRP bar (Degree)	CFRP bars spacing (mm)
Group1 with stirrups	G1-B1-Ref	-	-
	G1-B2-R-S10	90	100
	G1-B3-R-S15	90	150
	G1-B4-R-S20	90	200
	G1-B5-I-S10	45	100
	G1-B6-I-S15	45	150
	G1-B7-I-S20	45	200
Group2 without stirrups	G2-B1-Ref	-	-
	G2-B2-R-S10	90	100
	G2-B3-R-S15	90	150
	G2-B4-I-S10	45	100
	G2-B5-I-S15	45	150

brick element (C3D8R) to depict the concrete material accurately. The three-dimensional two-node bar element having three-dimensional motions in the x, y, and z dimensions, known as the truss element (T3D2), was used for the reinforced steel bars or CFRP bars. Many components were generated to fully analyze all specimens inside the ABAQUS environmental framework, as seen in **Fig. 3**.

Table 2. Properties of CFRP bars.

Product name	Sika® CarboDur® BC rods
Tensile strengths (MPa)	3100
E- modulus (GPa)	148
Breaking strain (min.) %	1.70
Diameter (mm)	12
Weight (kg/m)	≤ 0.32

The beam with one edge simply supported is simulated as a hinge by restricting the nodes along one line of supporting plate in tandem with the beam soffit's breadth in the local x-y directions (Ux=Uy=0).
In contrast, the other support is treated as a roller by restricting the y-direction (Uy=0) and permitting longitudinal motions and rotations around the x-axis. **Fig. 4** shows the boundary conditions and load definitions. **Table 3** presents the input data material for concrete

plasticity properties. The reinforcement steel and CFRP bars are considered entirely embedded in concrete to evaluate the complete interaction.

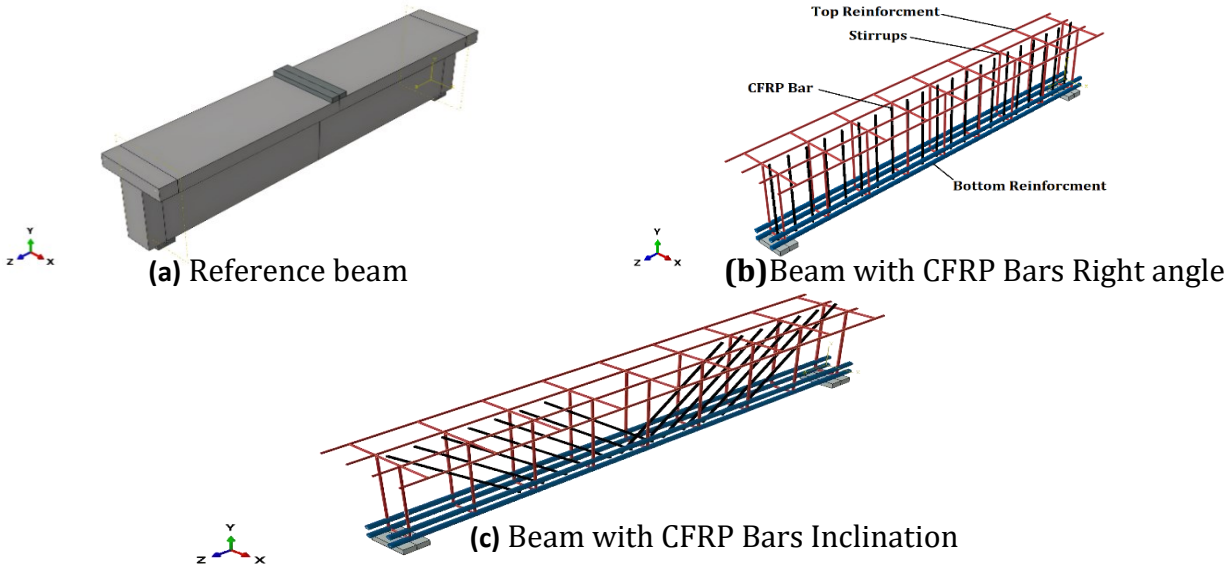

(a) Reference beam **(b)**Beam with CFRP Bars Right angle

(c) Beam with CFRP Bars Inclination

Figure 3. Creating parts and assembly in ABAQUS, **a)** Reference beam., **b)** Beam with CFRP Right angle, **c)** Beam with CFRP Inclination

Table 3. Input data for concrete **(Zhang et al., 2010)****

property	value	property	value
Young's modulus*	28645 MPa	$\epsilon_{bo}/\epsilon_{co}$**	1.1666
Poisson ratio**	0.20	k_c**	0.667
Angle of dilation**	36.0	Viscosity parameter**	0
Eccentricity**	0.10	$Ec = 4700\sqrt{0.82 * 45.3}$	28645 MPa

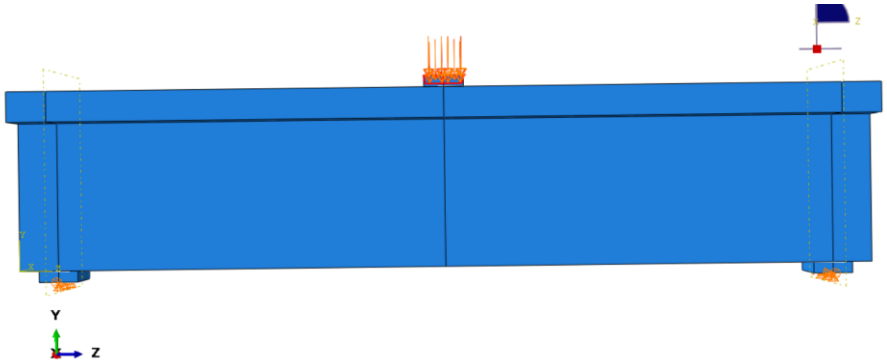

Figure 4. The utilized boundary and loading circumstances.

4. RESULT OF ANALYSIS OF TESTED BEAMS IN ABAQUS

4.1 Calibration of the Fabricated FE Model

Figs. 5 and 6 depict the load vs deflection relationship of the experimental and numerical results for the shear groups. Based on the finite element analysis findings, it has been determined that the models exhibit a higher degree of stiffness than the experimental samples. This conclusion is based on the observed load-deflection relations under the applied stresses. Increased stiffness in finite element method (FEM) analysis outcomes may be attributed to many causes. Cracks in the concrete were seen throughout the experimental procedure, arising from drying, shrinkage, and curing. Hence, it is possible for the total stiffness of the actual specimen to be lower than the anticipated stiffness determined from finite element (FE) analysis. **(Kachlakev et al., 2001).**

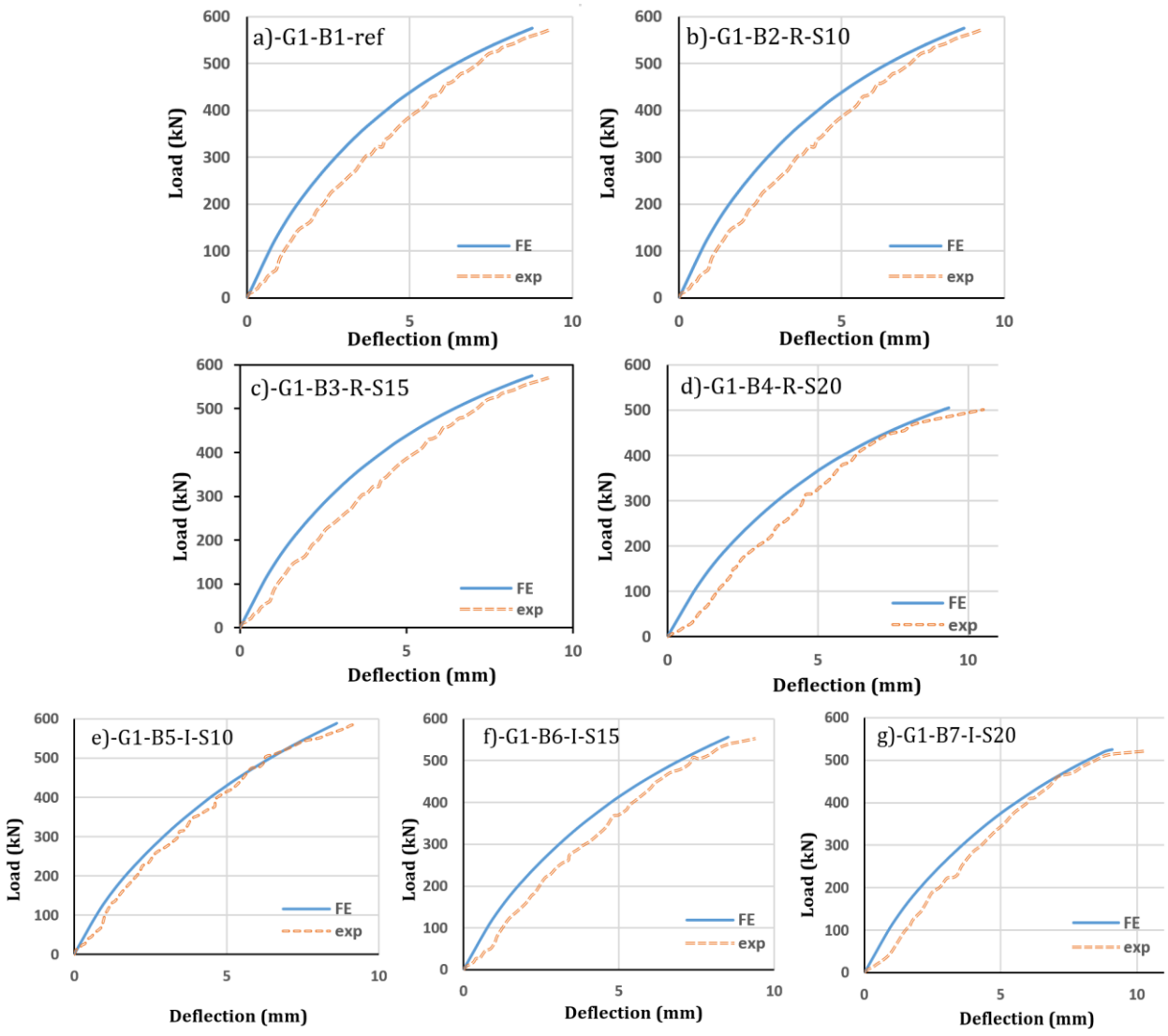

Figure 5. Load-deflection for the beams (group 1).

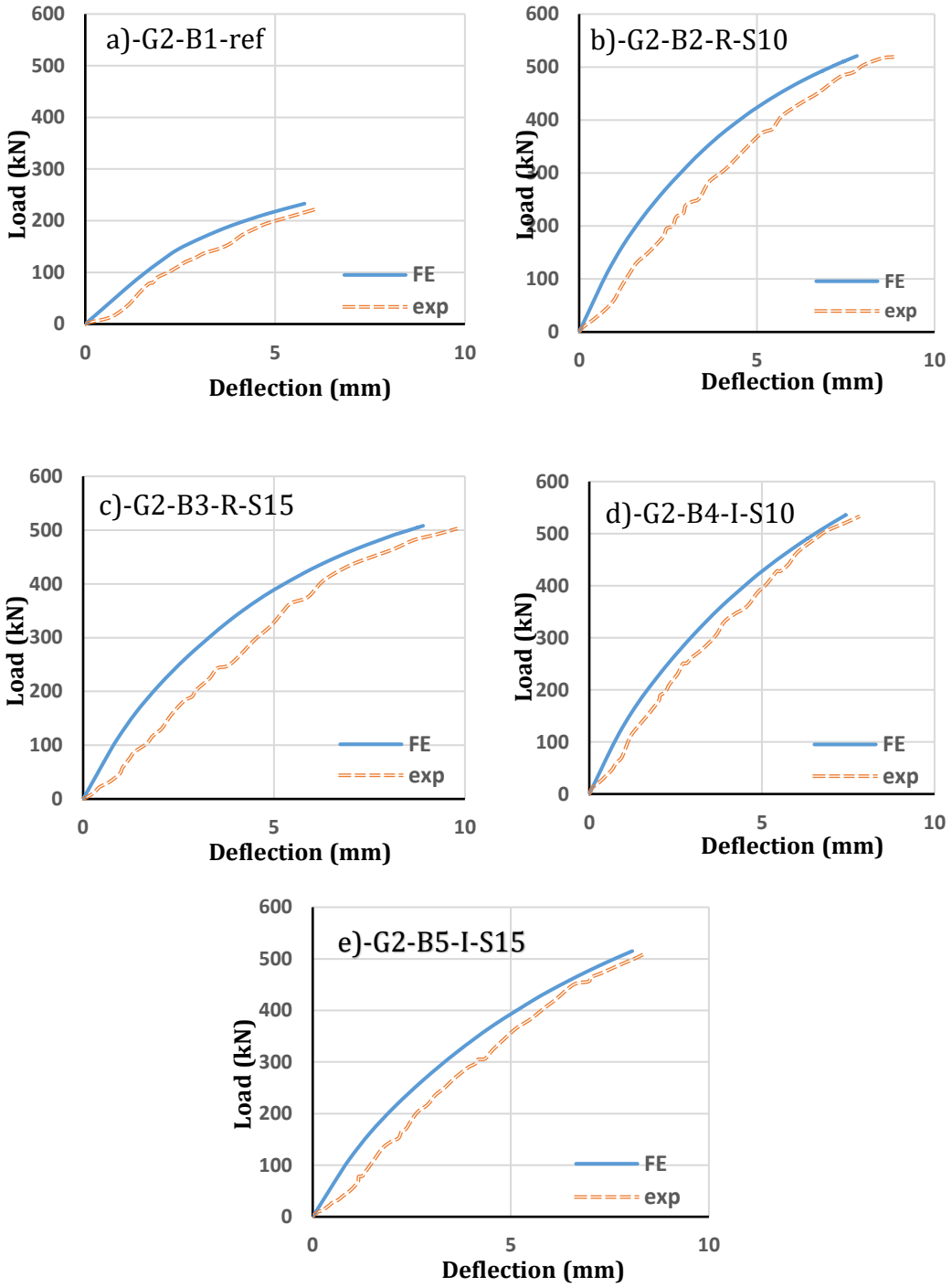

Figure 6. Load-deflection for the beams (group 2).

Table. 4 illustrates a comparative analysis of the failure load, the midpoint of a span deflection obtained from Abaqus, and the experimental test executed at the failure stage (close to the failing load) for all beams submitted to static testing. A strong correlation was

observed between the Abaqus models' ultimate loads and deflection and those obtained through practical means. Specifically, the mean and coefficient of variation for the ratio of ultimate loads (Pu)FE/(Pu)Exp were determined to be 1.011 and 1.336%, respectively. Similarly, for the ratio of deflection (δ FE / δ Exp), the average value and coefficient of variation were discovered to be 0.928 and 3.464%, respectively. Therefore, finite element analysis may be considered a preferred and reliable method for modeling the nonlinear behavior of RC T-beams with CFRP bars.

Table 4. Failure load and mid-span deflection.

Beam		Maximum Load (Pu)			Deflection at maximum load (Δu)		
		EXP (kN)	FE (kN)	FE/EXP	EXP (mm)	FE (mm)	FE/EXP
Group 1 (with stirrups)	G1-B1-Ref	451	455	1.00887	8.33	8.15	0.9784
	G1-B2-R-S10	570	575	1.0088	9.23	8.76	0.949
	G1-B3-R-S15	535	540	1.009	10.08	9.21	0.9137
	G1-B4-R-S20	501	505	1.00798	10.5	9.36	0.891
	G1-B5-I-S10	585	588	1.0051	9.18	8.61	0.9379
	G1-B6-I-S15	552	556	1.007	9.35	8.51	0.9101
	G1-B7-I-S20	521	525	1.0077	10.25	9.1	0.8878
Group 2 (without	G2-B1-Ref	221	233	1.05429	6.01	5.78	0.9617
	G2-B2-R-S10	519	521	1.00385	8.81	7.82	0.8876
	G2-B3-R-S15	502	508	1.01195	9.76	8.9	0.9118
	G2-B4-I-S10	532	536	1.00751	7.79	7.43	0.9537
	G2-B5-I-S15	510	515	1.0098	8.39	8.07	0.9618
Mean				1.011	Mean		0.928
Coef. of variation (%)				1.336	Coef. of variation (%)		3.464

4.2 Crack Patterns

It is advised to use a damage model in conjunction with a plasticity model, which is rooted in the principles of continuum damage mechanics, to forecast and simulate the behavior of concrete accurately **(Hafezolghorani et al., 2017; Yang et al., 2018; Raza and Ahmad, 2019; Al-Zuhairi et al., 2022; Tran et al., 2023)**.

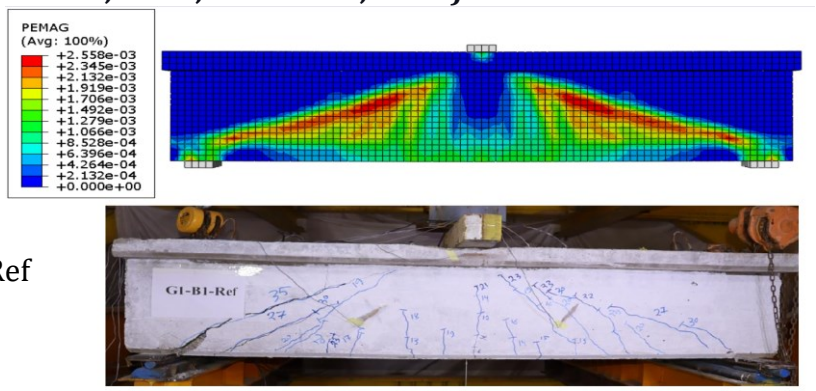

a)- G1-B1-Ref

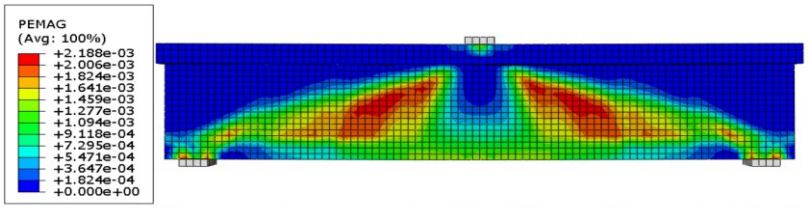

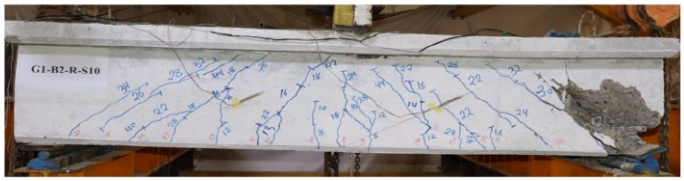

b)- G1-B2-R-S10

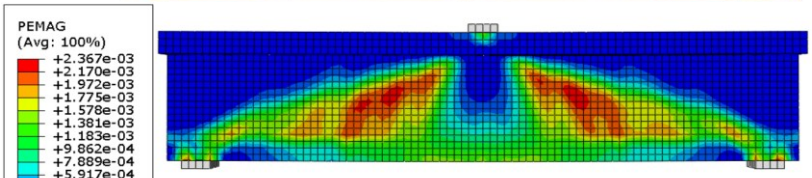

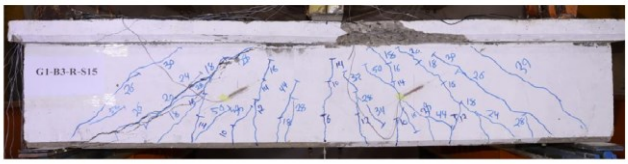

c)- G1-B3-R-S15

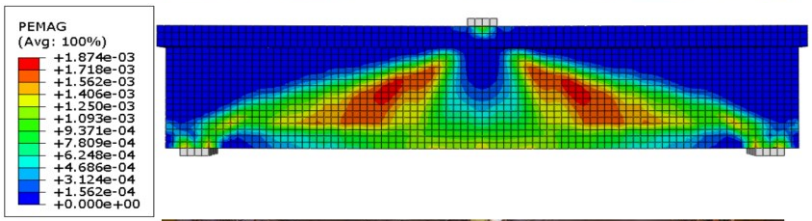

d)- G1-B4-R-S20

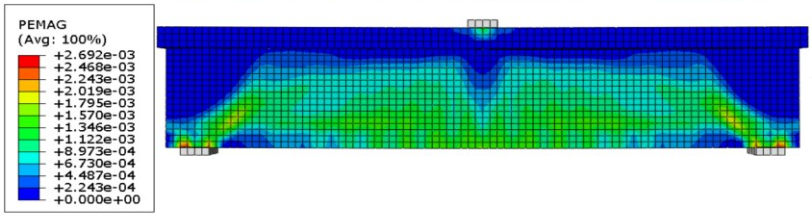

e)- G1-B5-I-S10

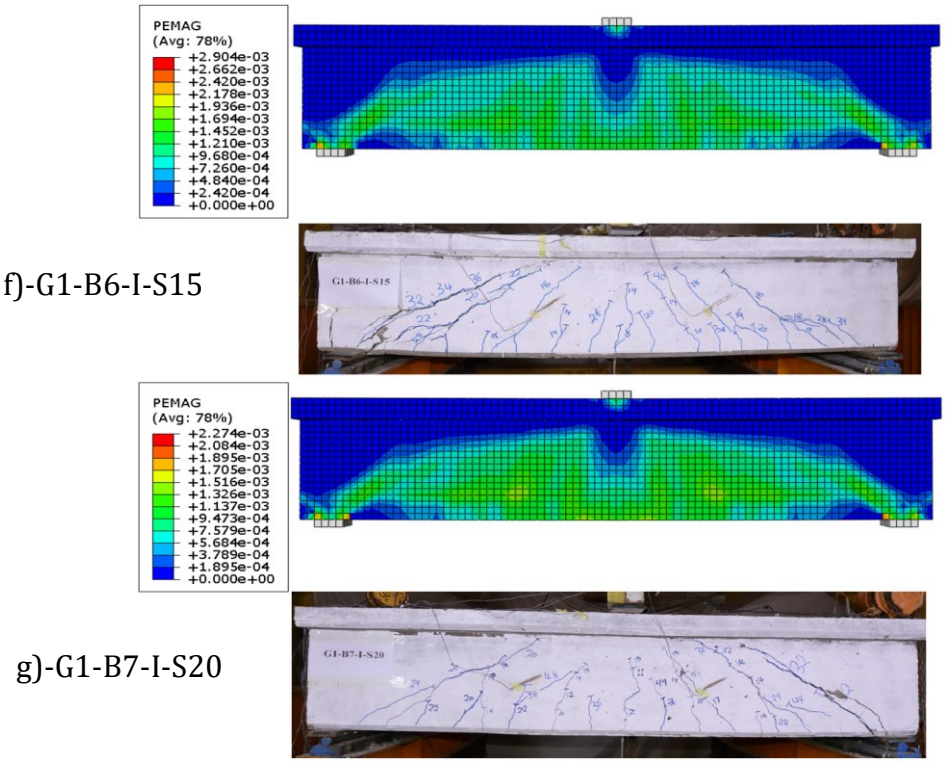

f)-G1-B6-I-S15

g)-G1-B7-I-S20

Figure 7. Ultimate cracking of the ABAQUS and experimental model (group one).

The correct simulation of concrete behavior in a damaged-plasticity model may be achieved by defining parameters such as compressive and tensile damage. Based on the CDP theory, cracks in RC members are commonly formed in zones where the tensile strain exists. More than the specified tensile strain of concrete, i.e., concrete would have cracked when the plastic strain exceeds zero. As a result, in the current investigation, the plastic strain was employed as a representative for crack expansion **(Mahmud et al., 2013; Faron et al., 2020; Raza et al., 2020; Daneshvar et al., 2022; Faron et al., 2023)**. The cracks are thought to be orthogonal to the max-plastic strain. **Figs. 7 and 8** show a contour plot of the max-plastic strain in the studied beams and the crack patterns of the experimental beams at the final stage for groups one and two, respectively, illustrating the impact of strengthening on strain concentrations and crack patterns. It is clear from these figures that shear failure was observed in all beams.

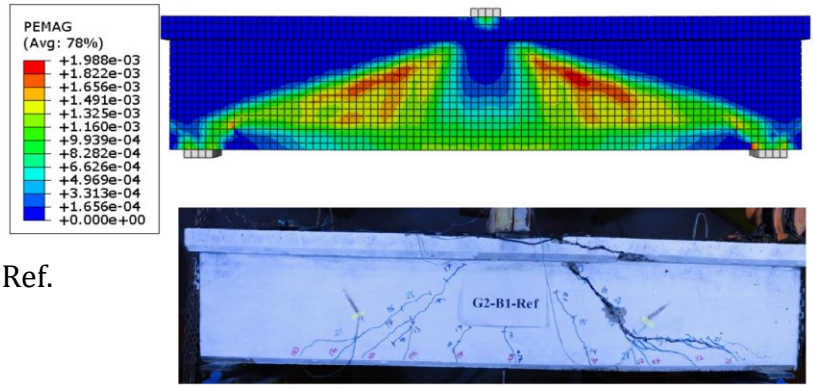

a)- G2-B1-Ref.

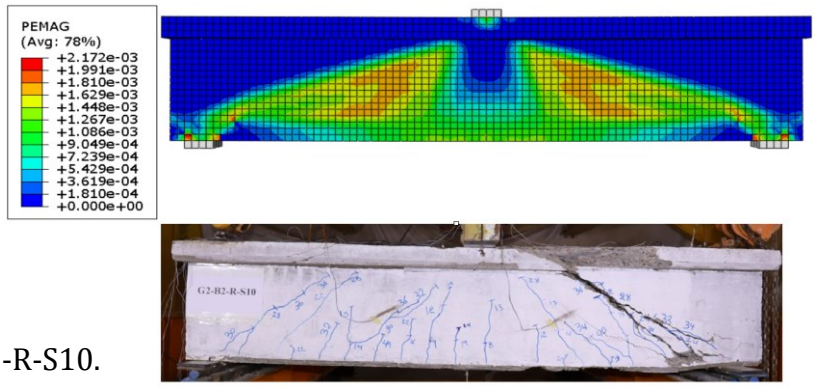

b)- G2-B2-R-S10.

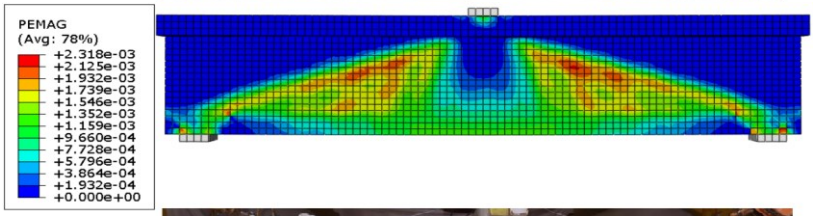

c)- G2-B3-R-S15

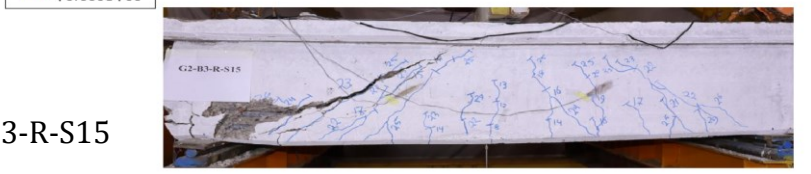

d)- G2-B4-I-S10

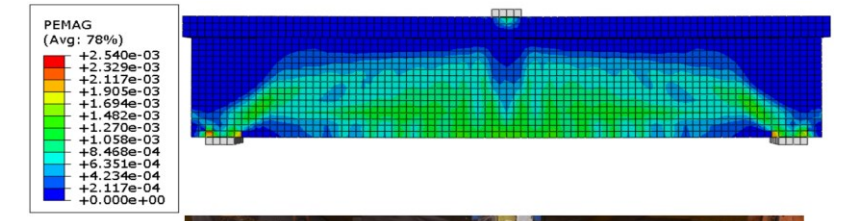

e)- G2-B5-I-S15

Figure 8. Ultimate cracking of the ABAQUS and experimental model (group two).

4.3 A Comparison Between the Experimental and FEM Diagonal Strain

Figs. 9 and 10 show a comparison between the diagonal strain of the experimental (tested) and FEM for all beams. There was a clear convergence between the experimental and numerical curves.

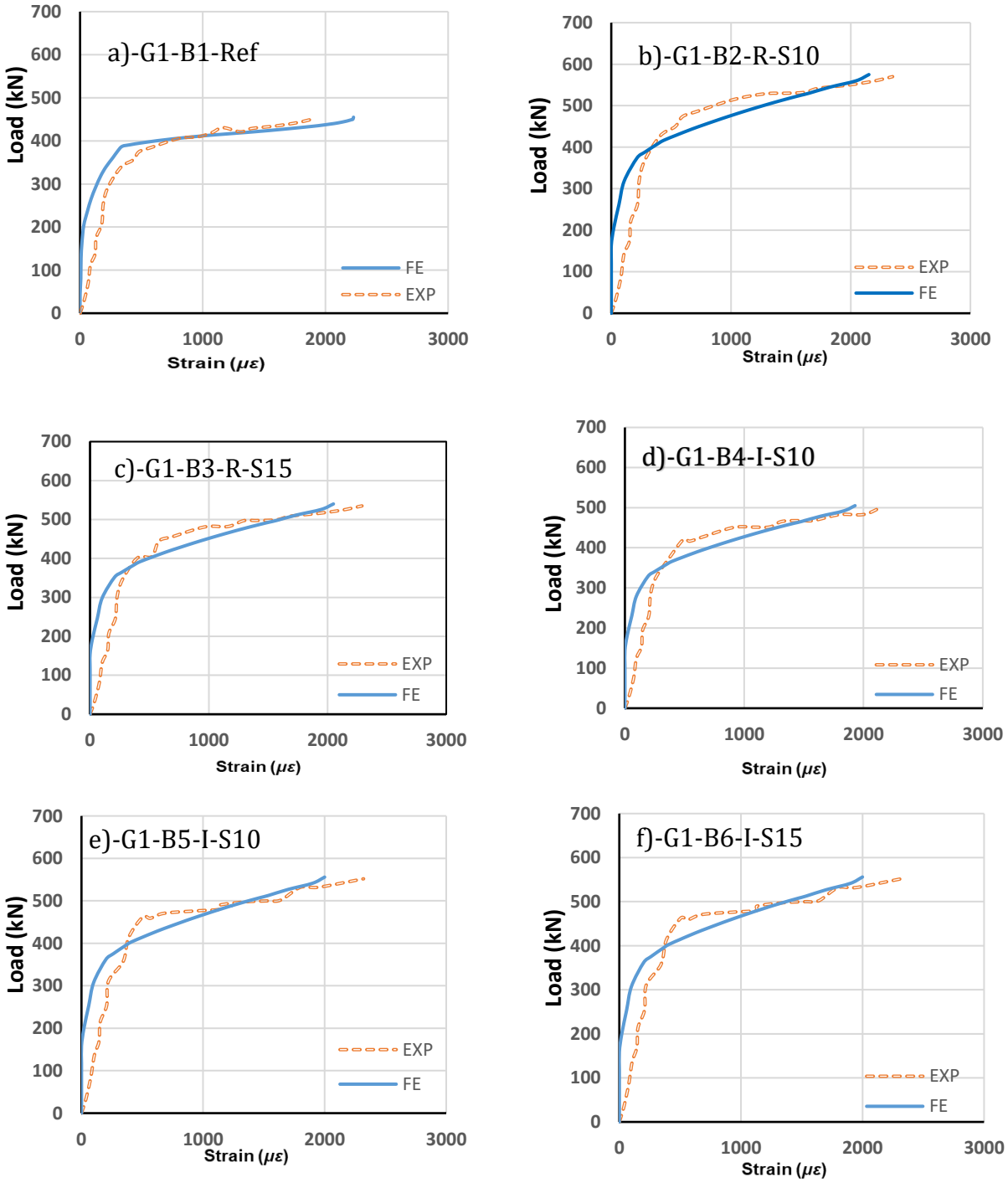

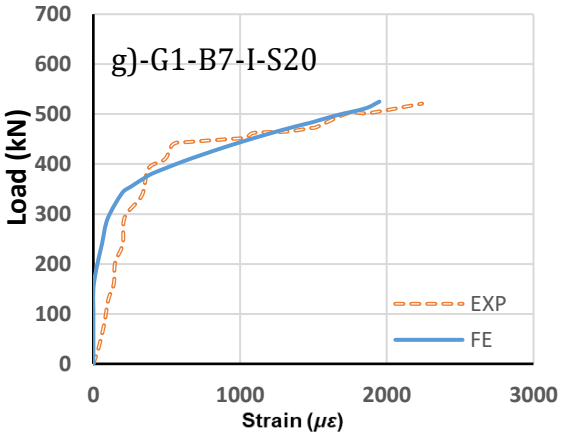

Figure 9. A comparison between the tested and FEM diagonal strain for group 1.

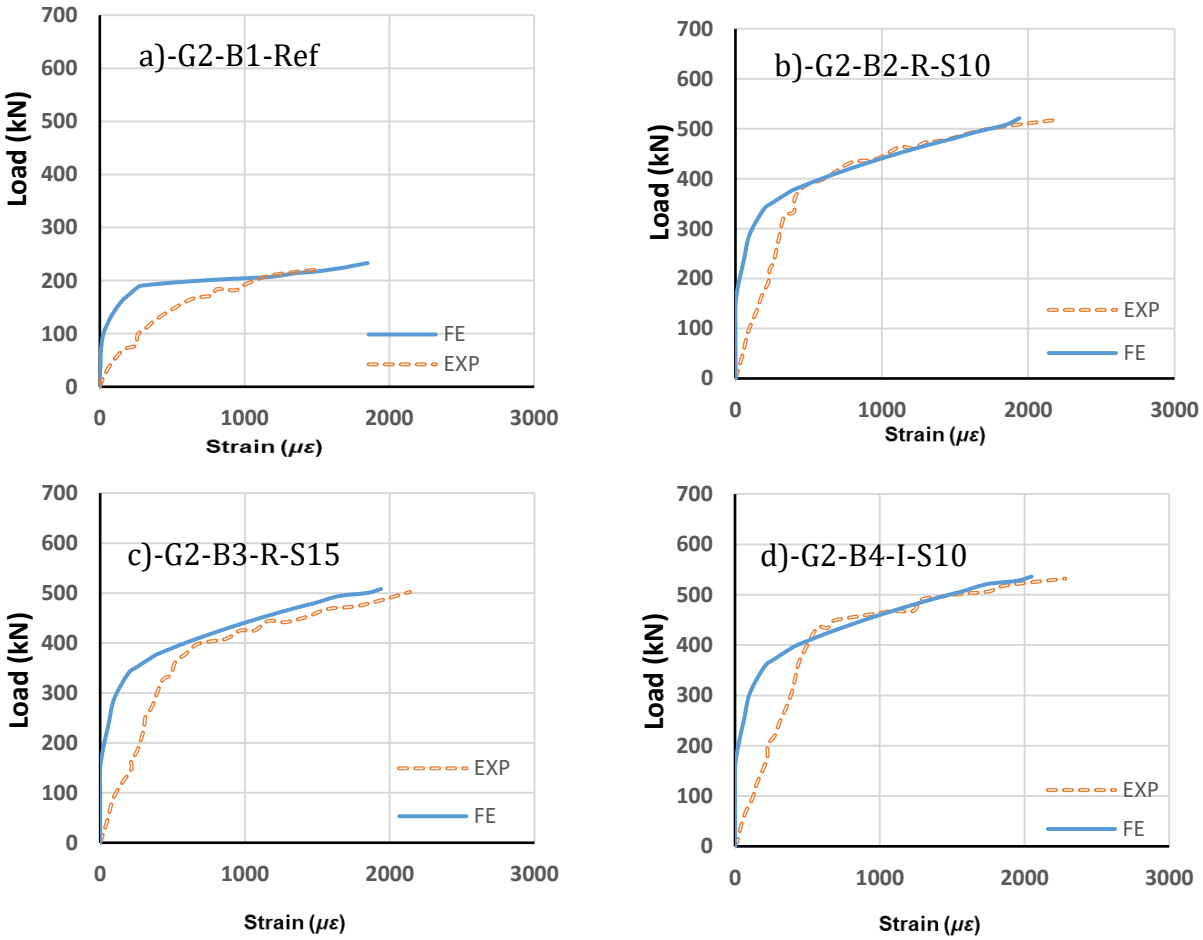

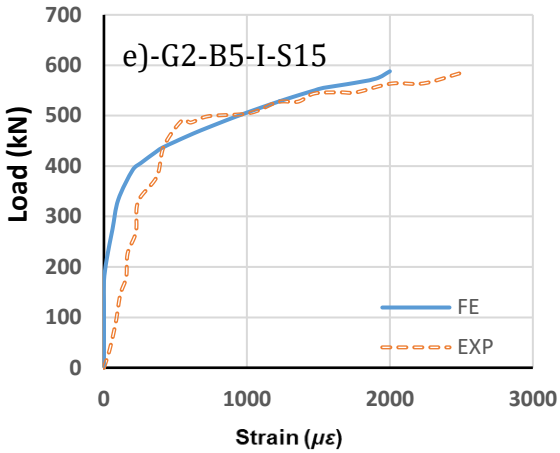

Figure 10. A comparison between the tested and FEM diagonal strain for group 2.

4.4 Numerical Parametric Study

Considering the preceding verification of the finite element evaluation for the experimental data obtained in this work, a comprehensive parametric study was conducted using the FE model. The investigation parameter is the diameter of the CFRP bar. The effect of the diameter of CFRP bar on the beam's structural behavior was studied for six previous models of group1 (G1-B2-R-S10, G1-B3-R-S15, G1-B4-R-S20, G1-B5-I-S10, G1-B6-I-S15 and G1-B7-I-S20,) in addition to twelve new models as shown in **Table. 5**.

Table 5. Details of beams for numerical parametric study.

Beam-ID	angle of inclination of CFRP bar (Degree)	CFRP bars spacing (mm)	CFRP bars diameter (mm)
G1-B2-R-S10	90	100	12
G1-B3-R-S15	90	150	12
G1-B4-R-S20	90	200	12
G1-B5-I-S10	45	100	12
G1-B6-I-S15	45	150	12
G1-B7-I-S20	45	200	12
G1-B2-R-S10-10	90	100	10
G1-B3-R-S15-10	90	150	10
G1-B4-R-S20-10	90	200	10
G1-B5-I-S10-10	45	100	10
G1-B6-I-S15-10	45	150	10
G1-B7-I-S20-10	45	200	10
G1-B2-R-S10-16	90	100	16
G1-B3-R-S15-16	90	150	16
G1-B4-R-S20-16	90	200	16
G1-B5-I-S10-16	45	100	16
G1-B6-I-S15-16	45	150	16
G1-B7-I-S20-16	45	200	16

The influence of changing the diameter of the CFRP bar (10,12,16mm) on the load vs deflection relationship at the middle span point is depicted in **Fig. 11**. Each figure has beams with the same spacing and inclination of CFRP bars. From load vs deflection curves, it is evident that the beams exhibit equal stiffness throughout the elastic range after the occurrence of cracking. The beams with a higher diameter of the CFRP bar have higher shear stiffness.

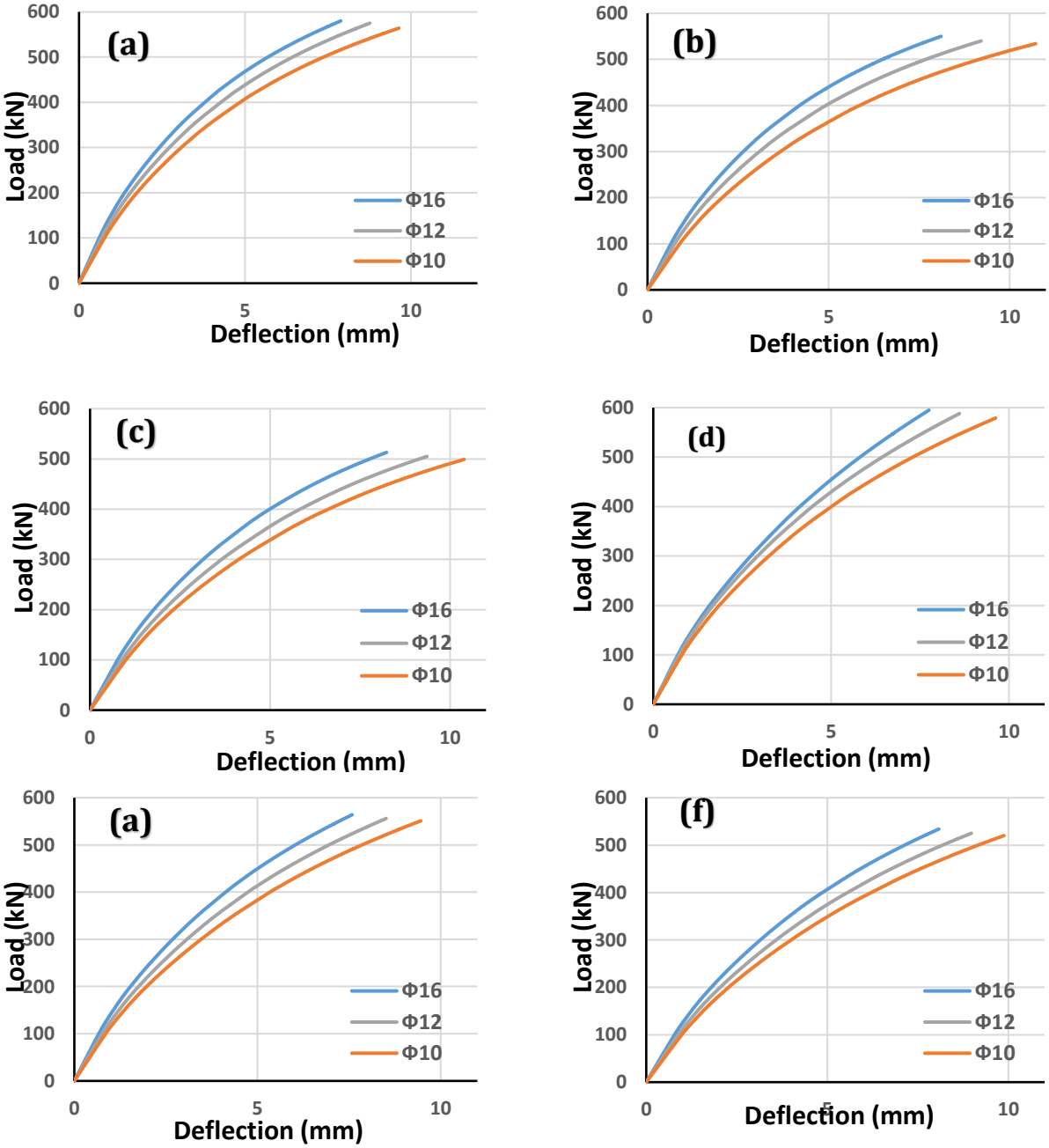

Figure 11. load-deflection for the numerical parametric study, a) beams with bars 90 and spacing 100mm, b) beams with bars 90 and spacing 150mm, c) beams with bars 90 and spacing 200mm, d) beams with bars 45 ° and spacing 100mm, e) beams with bars 45 ° and spacing 150mm, f) beams with bars 45 ° and spacing 200mm

As given in **Table. 6**, for the beams with a CFRP bar diameter of 12mm, the ultimate load increases by 26.4, 18.7, and 11%; for beams with vertical CFRP bars and spacing of 100, 150, and 200mm, respectively, concerning the reference beam, and by 29.2, 22.2, and 15.4 for the beam with inclined CFRP bars and a spacing of 100, 150, and 200mm respectively concerning the reference beam. For the beams with a CFRP bar diameter of 100mm, the ultimate load increases by 24, 17.4, and 9.7%; for a beams with vertical CFRP bars and a spacing of 100, 150, and 200mm, respectively, concerning the reference beam, and by 27.3, 21.1, and 14.3 for the beam with inclined CFRP bars and a spacing of 100, 150, and 200mm respectively concerning the reference beam. For the beams with a CFRP bar diameter of 16mm, the ultimate load increases by 27.5, 20.9, and 12.8%; for beams with vertical CFRP bars and a spacing of 100, 150, and 200mm, respectively, concerning the reference beam, and by 30.8, 24, and 17.4 for the beam with inclined CFRP bars and a spacing of 100, 150, and 200mm respectively concerning the reference beam.

Table 6. The ultimate load of beams for numerical parametric study.

Beam-ID	angle of inclination of CFRP bar (Degree)	CFRP bars spacing (mm)	CFRP bars diameter (mm)	$Pu=P_{ultimate}$ (kN)	Increase of Pu related to Pu of reference (%)
G1-B1-Ref	-	-	-	455	Ref.
G1-B2-R-S10	90	100	12	575	26.4
G1-B3-R-S15	90	150	12	540	18.7
G1-B4-R-S20	90	200	12	505	11
G1-B5-I-S10	45	100	12	588	29.2
G1-B6-I-S15	45	150	12	556	22.2
G1-B7-I-S20	45	200	12	525	15.4
G1-B2-R-S10-10	90	100	10	564	24
G1-B3-R-S15-10	90	150	10	534	17.4
G1-B4-R-S20-10	90	200	10	499	9.7
G1-B5-I-S10-10	45	100	10	579	27.3
G1-B6-I-S15-10	45	150	10	551	21.1
G1-B7-I-S20-10	45	200	10	520	14.3
G1-B2-R-S10-16	90	100	16	580	27.5
G1-B3-R-S15-16	90	150	16	550	20.9
G1-B4-R-S20-16	90	200	16	513	12.8
G1-B5-I-S10-16	45	100	16	595	30.8
G1-B6-I-S15-16	45	150	16	564	24
G1-B7-I-S20-16	45	200	16	534	17.4

5. CONCLUSIONS

This work presents strengthening beams in shear failure by used CFRP bars embedded through a section, using two groups in this research, each group included two variables, a spacing and angle of inclination of CFRP bar, in this paper study, correspond between the experimental work and numerical, and compare both of them.

1. There was a significant connection found between the ultimate loads and deflection of the computer data and the results from experimental methods. More specifically, the average and variation coefficient for the ultimate load ratio (Pu)FE/(Pu)Exp were calculated as 1.011 and 1.336%, respectively. In the same way, the average and variability coefficient for the deflection ratio (δ FE / δ Exp) were found to be 0.928 and 3.464%, respectively.
2. The beam stiffness is directly related to the diameter of the CFRP bars when the angle of inclination and spacing remain constant.
3. The impact of changing the CFRP bar diameter on the ultimate load was small, where the ultimate load of all beams increases by 0.91 to 1.95% for beams with a CFRP bar diameter of 12mm, concerning the similar beam with a CFRP bar diameter of 10mm. And the ultimate load of all beams increases by 2.4 to 3% for beams with a CFRP bar diameter of 16mm, and similar beams with a CFRP bar diameter of 10mm.
4. The beam stiffness is inversely correlated to the increased spacing of the CFRP bars at the same degree of inclination.
5. There was a clear convergence between the experimental and numerical of load vs diagonal strain curves.

NOMENCLATURE

Symbol	Description	Symbol	Description
RC	Reinforced concrete	C3D8R	Isoperimetric eight-node brick element
CFRP	Carbon fiber reinforced polymer	T3D2	Three dimensional two-node bar element
ETS	Embedded through section	FEM	Finite element method
EB	External bonded	Pu	Ultimate load
NSM	Near surface mounted	CDP	Concrete Damage Plasticity
FRP	Fiber reinforced polymer	f'c	compressive strength of concrete
DE	Deep embedment	a/d	Ratio of shear span

Acknowledgements

The authors thank the cooperation of the civil engineering department at the University of Baghdad for supporting the experimental work conducted in this research.

Credit Authorship Contribution Statement

Hussain Hassan Alhilli: Writing–original draft, Validation, Methodology. Mahdi Hameed Al-Farttoosi: Review & editing, Proofreading.

Declaration of Competing Interest

The authors declare that they have no known competing financial interests or personal relationships that could have appeared to influence the work reported in this paper.

REFERENCES

Abbas, H. Q., and Al-Zuhairi, A. H., 2023. Impact of anchored CFRP composites on the strengthening of partially damaged PC girders. *Journal of Engineering*, *29*(8), pp. 106-120. https://doi.org/10.31026/j.eng.2023.08.08

Abbas, S. A., Izzat, A. F., and Farhan, J. A., 2013. Retrofitting reinforced concrete one–way damaged slabs exposed to high temperature. *Journal of Engineering*, *19*(07), pp. 845-862. https://doi.org/10.31026/j.eng.2013.07.06

Abbasi, A., Benzeguir, Z. E. A., Chaallal, O., and El-Saikaly, G., 2022. FE modelling and simulation of the size effect of RC T-beams strengthened in shear with externally bonded FRP fabrics. *Journal of Composites Science*, *6*(4), pp. 116. https://doi.org/10.3390/jcs6040116.

Abdulkareem, B.F., and Izzat, A.F., 2022. Serviceability of post-fire RC rafters with openings of different sizes and shapes. *Journal of Engineering*, *28*(1), pp. 19-32. https://doi.org/10.31026/j.eng.2022.01.02.

Al-Farttoosi, M., Rafiq, Y., Summerscales, J. and Williams, C., 2013. Nonlinear finite element analysis (fea) of flexural behavior of reinforced concrete beams externally strengthened with CFRP. *Advanced Composites in Construction (ACIC) 2013 Conference Proceedings*.

Al-Zuhairi, A. H., Al-Ahmed, A. H., Abdulhameed, A. A., and Hanoon, A. N., 2022. Calibration of a new concrete damage plasticity theoretical model based on experimental parameters. *Civil Engineering Journal*, *8*(2), pp. 225-237. http://dx.doi.org/10.28991/CEJ-2022-08-02-03.

Alhilli, H.H. and Al-Farttoosi, M.H., 2023. Shear performance of reinforced concrete t beams strengthened by carbon fiber-reinforced polymer bars. *Civil Engineering Journal*, *9*(10), pp.2411-2429. http://dx.doi.org/10.28991/CEJ-2023-09-10-04.

Benzeguir, Z.E., El-Saikaly, G. and Chaallal, O., 2019. Size effect in RC T-beams strengthened in shear with externally bonded CFRP sheets: Experimental study. *Journal of Composites for Construction*, 23(6). https://doi.org/10.1061/(asce)cc.1943-5614.0000975.

Buyukozturk, O., Gunes, O., and Karaca, E., 2004. Progress on understanding debonding problems in reinforced concrete and steel members strengthened using FRP composites. *Construction and Building Materials*, 18(1), pp. 9-19. https:\doi.org\10.1016\S0950-0618(03)00094-1.

Barros, Joaquim AO, and G. M. Dalfré., 2013. Assessment of the effectiveness of the embedded through-section technique for the shear strengthening of reinforced concrete beams. *Strain*, 49(1), pp. 75-93. https://doi.org/10.1111/str.12016

Chaallal O., Mofidi A., Benmokrane B., and Neale K., 2011. Embedded through-section FRP rod method for shear strengthening of RC beams: Performance and comparison with existing techniques. *Journal of composites for construction,* 15(3), pp. 374-383. https://doi.org/10.1061/(ASCE)CC.1943-5614.0000174.

Chen, H., Yi, W.J., Ma, Z.J. and Hwang, H.J., 2019. Shear Strength of Reinforced Concrete Simple and Continuous Deep Beams. *ACI Structural Journal*, *116*(6). https://doi.org/10.14359/51718003

Daneshvar, K., Moradi, M. J., Khaleghi, M., Rezaei, M., Farhangi, V., and Hajiloo, H., 2022. Effects of impact loads on heated-and-cooled reinforced concrete slabs. *Journal of Building Engineering*, 61(1), P. 105328. https://doi.org/10.1016/j.jobe.2022.105328.

Deniaud, C., and Roger Cheng, J. J., 2003. Reinforced concrete T-beams strengthened in shear with fiber reinforced polymer sheets. *Journal of Composites for Construction*, *7*(4), pp. 302-310. https://doi.org/10.1061/(ASCE)1090-0268(2003)7:4(302).

Faron, A., and Rombach, G. A., 2020. Simulation of crack growth in reinforced concrete beams using extended finite element method. *Engineering Failure Analysis*, 116(1), pp. 104698. https://doi.org/10.1016/j.engfailanal.2020.104698.

Faron, A., and Rombach, G. A., 2023. Discrete crack propagation analysis of reinforced concrete beams under shear. *In AIP Conference Proceedings*, 2848(1), AIP Publishing. https://doi.org/10.1063/5.0145044%20.

Feng, D. C., Ren, X. D., and Li, J., 2018. Softened damage-plasticity model for analysis of cracked reinforced concrete structures. *Journal of Structural Engineering*, 144(6), pp. 04018044. https://doi.org/10.1061/(ASCE)ST.1943-541X.0002015.

Ghadhban, Hadi Nasir., 2007. Effect of beam size on shear strength of reinforced concrete normal beams. *Journal of Engineering and Development*, 11(1).

Godat, Ahmed, Omar Chaallal, and Kenneth W. Neale., 2013. Nonlinear finite element models for the embedded through-section FRP shear-strengthening method. *Computers and Structures,* 119(1), pp. 12-22. https://doi.org/10.1016/j.compstruc.2012.12.016.

Hafezolghorani, M., Hejazi, F., Vaghei, R., Jaafar, M. S. B., and Karimzade, K., 2017. Simplified damage plasticity model for concrete. *Structural Engineering international*, 27(1), pp. 68-78. https://doi.org/10.2749/101686616X1081.

Izzat, A. F., 2015. Retrofitting of reinforced concrete damaged short column exposed to high temperature. *Journal of Engineering*, *21*(3), pp. 34-53. https://doi.org/10.31026/j.eng.2015.03.03.

Kachlakev, D. I., Miller, T. H., Potisuk, T., Yim, S. C., and Chansawat, K., 2001. Finite element modeling of reinforced concrete structures strengthened with FRP laminates. (No. FHWA-OR-RD-01-XX). Oregon. Dept. of Transportation. Research Group. https://rosap.ntl.bts.gov/view/dot/23018.

Mahmud, G. H., Yang, Z., and Hassan, A. M., 2013. experimental and numerical studies of size effects of ultra high performance steel fiber reinforced concrete (UHPFRC) beams. *Construction and Building Materials*, 48(1), pp. 1027-1034. http://dx.doi.org/10.1016/j.conbuildmat.2013.07.061.

Mhanna, Haya H., Rami A. Hawileh, and Jamal A. Abdalla., 2019. Shear strengthening of reinforced concrete beams using CFRP wraps. *Procedia Structural Integrity*, 17 (1), pp. 214-221. https://doi.org/10.1016/j.prostr.2019.08.029.

Najaf, E., Orouji, M., and Ghouchani, K., 2022. Finite element analysis of the effect of type, number, and installation angle of FRP sheets on improving the flexural strength of concrete beams. *Case Studies in Construction Materials*, 17(1). https://doi.org/10.1016/j.cscm.2022.e01670.

Naqe, A. W., and Al-zuhairi, A. H., 2020. Strengthening of RC beam with large square opening using CFRP. *Journal of Engineering*, *26*(10), pp. 123-134. https://doi.org/10.31026/j.eng.2020.10.09.

Naqi, Aya Waleed, and Alaa H. Al-zuhairi., 2020. Nonlinear finite element analysis of RCMD beams with large circular opening strengthened with CFRP material. *Journal of Engineering,* 26 (11), pp. 170-183. https://doi.org/10.31026/j.eng.2020.11.11.

Qapo, M., Dirar, S., and Jemaa, Y., 2016. Finite element parametric study of reinforced concrete beams shear-strengthened with embedded FRP bars. *Composite Structures*, 149(1), pp. 93-105. https://doi.org/10.1016/j.compstruct.2016.04.017.

Raza, A., and Ahmad, A., 2019. Numerical investigation of load-carrying capacity of GFRP-reinforced rectangular concrete members using CDP model in ABAQUS. *Advances in Civil Engineering*. https://doi.org/10.1155/2019/1745341.

Raza, A., and Khan, Q. U. Z., 2020. Experimental and numerical behavior of hybrid-fiber-reinforced concrete compression members under concentric loading. *SN Applied Sciences*, 2(4), pp. 701. https://doi.org/10.1007/s42452-020-2461-5.

Tran, D. A., Shen, X., Sorelli, L., Ftima, M. B., and Brühwiler, E., 2023. Predicting the effect of non-uniform fiber distribution on the tensile response of ultra-high-performance fiber reinforced concrete by magnetic inductance-based finite element analysis. *Cement and Concrete Composites*, 135(1), pp. 104810. https://doi.org/10.1016/j.cemconcomp.2022.104810.

Turki, A. Y., and Al-Farttoosi, M. H., 2023. Flexural strength of damaged RC beams repaired with carbon fiber-reinforced polymer (CFRP) using different techniques. *Fibers*, 11(7), pp. 61. https://doi.org/10.3390/fib11070061.

Yang, X., Liu, L., and Wang, Y., 2018. Experimental test and numerical simulation of the initial crack reinforced concrete beam in bending. *In IOP Conference Series: Earth and Environmental Science*, 186(2), pp. 012056. https://doi.org/10.1088/1755-1315/186/2/012056.

Zhang, J., Zhang, Z., and Chen, C., 2010. Yield criterion in plastic-damage models for concrete. *Acta Mechanical Solida Sinica*, 23(3), pp. 220–230. https://doi.org/10.1016/s0894-9166(10)60024-9.

التحليل بطريقة العناصر المحددة لأداء القص للعتبات الخرسانية ذات مقطعT المسلحة بقضبان البوليمر المقواة بالياف الكاربون بتقنية الاندماج في المقطع

حسين حسن الحلي*، مهدي حميد الفرطوسي

قسم الهندسة المدنية، كلية الهندسة، جامعة البصرة، البصرة، العراق

الخلاصة

تعرض هذه الورقة نتائج البحث التي تم الحصول عليها من المحاكاة العددية التي أجريت باستخدام برنامج العناصر المحدودة ABAQUS/CAE الإصدار 2019. كان الهدف من هذه الدراسة هو دراسة أداء القص للعتبات T المبنية من الخرسانة المسلحة (RC) والمعززة بقضبان البوليمر المقوى بألياف الكربون (CFRP) والتي تم دمجها من خلال المقطع (ETS). تضمن نهج التحقق العددي تطبيق التحليل العددي على البيانات التجريبية التي تم الحصول عليها من اثني عشر عارضة من الخرسانة المسلحة (RC). وبعد ذلك، تم توسيع نطاق التحليل العددي ليشمل دراسة الجوانب الأخرى، بما في ذلك تأثير قطر قضبان البوليمر المقوى بألياف الكربون. الهدف الأساسي من هذا المشروع هو تطوير نموذج حسابي قادر على تكرار الخصائص غير الخطية المعقدة المتأصلة في الحزم بأمانة. تجري هذه الدراسة تحليلًا مقارنًا للنماذج الحسابية والتجريبية، مع التركيز بشكل خاص على خصائص انحراف الحمل وأنماط التشقق. وتظهر النتائج درجة كبيرة من الاتفاق بين المنهجيتين. أشارت الدراسة إلى أن متوسط نسبة الحمل النهائي إلى الانحرافات في نماذج المحاكاة العددية والاختبارات التجريبية للعتبات كانت 1.011 و0.928 على التوالي. أظهرت نتائج البحث وجود علاقة مباشرة بين قطر قضبان البوليمر المقوى بألياف الكربون وصلابة العتبة، في ظل افتراض وجود زاوية ميل وتباعد ثابتة.

الكلمات المفتاحية: عتبات تي، قضبان البوليمر المقوى بالألياف الكربونيةCFRP، اجهادات القص، المدمجة من خلال المقطع (ETS).